Paper presented at 9th International Pulsed Power Conference
Albuquerque, June 21–23

TRI-PP-93-58
Jun 1993

A MATHEMATICAL MODEL OF A THREE-GAP THYRATRON SIMULATING TURN-ON

M.J. Barnes, G.D. Wait
TRIUMF, 4004 Wesbrook Mall, Vancouver, B.C., Canada V6T 2A3

Abstract

Kicker magnets are required for all ring-to-ring transfers in the 5 rings of the proposed KAON factory synchrotron. The kick must rise/fall from 1% to 99% of full strength during the time interval of gaps created in the beam (80 ns to 160 ns) so that the beam can be extracted with minimum losses. Approximately one-third of the injection and extraction kicker magnets will operate continuously at a rate of 50 pulses per second: the others operate at 10 pulses per second. The kicker magnet PFN voltages will be in the range 50kV to 80kV, hence multi-gap thyratrons will be used for the injection and extraction kicker systems. Displacement current arising from turn-on of a multi-gap thyratron flows in the external circuit and can thus increase the effective rise-time of the kick. A mathematical model of a three-gap thyratron, which includes the drift spaces, has been developed for simulating turn-on, and is described in this paper. The thyratron model has been used to investigate ways to suppress the effects of displacement current on the kick, and to reduce thyratron switching loss. A ferrite saturating inductor may be connected adjacent to each thyratron to reduce the switching loss, so that thyratron life can be extended and the kick rise-time improved. This inductor can also be used to reduce the effect of anode displacement current during turn-on of a multi-gap thyratron. The research has culminated in a predicted kick rise time (1% to 99%) of less than 50 ns for a TRIUMF 10 cell prototype kicker magnet. The proposed improvements are currently being implemented on our prototype kicker system.

Introduction

Many of the kicker magnets for the proposed KAON factory synchrotron require kick rise/fall times of less than 82ns[1]. In order to achieve the required kick rise/fall times in the available space pulse forming network (PFN) voltages of approximately 50kV are typically required[1], hence multi-gap thyratrons are to be used for the high-voltage switches.

The design of the pulse generator proposed for the injection and extraction kicker magnets will be based on that of the CERN PS division[2, 3]: three gap deuterium filled thyratrons will be used for the high voltage switching. The individual gaps in a three gap thyratron break down in sequence[4, 5]. Initially the gap closest to the cathode conducts and the full PFN voltage is shared between the centre and anode gaps. Approximately 50ns later the centre gap starts to conduct and the full PFN voltage builds up across the anode gap[4]. The voltage redistribution between the parasitic capacitance of each of the gaps is associated with a flow of displacement current[5]. The displacement current also flows in the external circuit[5], and hence through the kicker magnet, and can increase the effective rise-time of the kick.

Fig. 2 of reference[1] shows a typical voltage pulse from a pulse generator borrowed from CERN PS Division: cathode displacement current, up to 5% of the magnitude of the flat-top, occurs for about 100ns before the main pulse. Anode displacement current causes a slight reduction in the flat-top of the measured pulse approximately 50ns before the tail begins[1].

Approximately one-third of the injection and extraction kicker magnets for the proposed KAON factory will operate continuously at a rate of 50 pulses per second: the others will operate at 10 pulses per second[1]. Switching loss in a thyratron operating at 50Hz is more important than in lower frequency applications[4]. Saturating ferrite cores connected adjacent to the anode of the thyratron may be be used to reduce the effect of anode displacement current[6], reduce switching loss[4], and improve current rise-time[4, 6].

In order to be able to investigate ways to suppress the effect of anode and cathode displacement current upon kick, and to reduce thyratron switching loss, a representative mathematical model of a thyratron has been developed. The circuit analysis code PSpice[7] is utilized for all the mathematical simulations whose results are reported in this paper.

Mathematical Model of a Thyratron Simulating Turn-On

Single Gap Thyratron Model

A non-linear switching characteristic for an EEV CX1168[8] thyratron simulating turn-on may be represented using the equivalent circuit shown in Fig. 1: this mathematical model is based on the CERN SPS Division's simulation of the CX1168[9]. Hsense and Hcontrol are both current-controlled voltage sources with unity gain, which are used for controlling voltage source Eproduct. The potential difference across the output terminals of Eproduct is given by the product of the current through Hsense and Hcontrol. ISA is a current source whose current decays exponentially, with time-constant τ_1, from a high-current (e.g. 50kA) to a low current (e.g. 20mA).

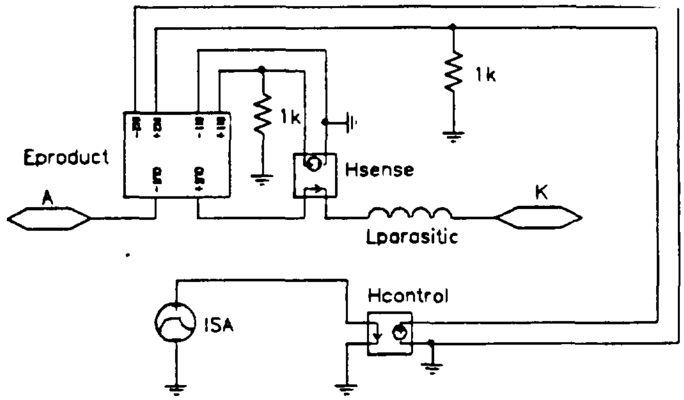

Figure 1: Equivalent circuit for generating a non-linear switching characteristic for a thyratron gap and/or drift space

The low current value of ISA can be chosen to give a representative conduction voltage drop at the required load current. This results in a simulated conduction voltage drop which is proportional to load current, which is not the situation in reality[4]. However, for the majority of simulations the resulting error is acceptable.

Lparasitic in Fig. 1 represents the parasitic inductance of a gap and/or drift space of a thyratron. The inductance of the CX1171 thyratron, in its coaxial housing, has been deduced to be 80nH[4].

Fig. 5 of reference[4] shows a thyratron current rise-time of about 33ns (10%→90%), for a reservoir voltage of 5.65 V and a PFN pre-charge of 80kV. Since the EEV CX1171 thyratron[8] used for the tests documented in reference[4] was manufactured in 1980, its rise time performance may be slower than that of currently produced tubes because of detail improvements[4]. A simulated value of 7ns for τ_1 results in a predicted 10% to 90% current rise-time of approximately 32ns for the equivalent circuit of Fig. 1.

Three Gap Thyratron Model

Figs. 2 and 3 show equivalent circuits for the CX1171[8] three-gap thyratron for simulating turn-on. The equivalent circuit of Fig. 2 simulates non-linear switching characteristics for three-gaps and two drift spaces. The equivalent circuit of Fig. 3 lumps the non-linear switching characteristics for the two drift spaces with those of the cathode and central gaps.

The 14MΩ resistors in Figs. 2 and 3 are for d.c. voltage grading[4]: the 540Ω resistors close the thyratron drift spaces[4]: Cgap represents the inter-electrode capacitance of each of the three gaps. The data sheet value for Cgap is 15pF to 20pF[8], and 20pF has been used throughout the reported simulations.

'XTHYRATRON' in Figs. 2 and 3 represents the equivalent circuit shown in Fig. 1. Analysis of measured anode, cathode and gradient grid voltages during turn-on of a multi-gap thyratron, indicates that the time duration associated with the collapse of voltage across a gap is similar for all the gaps[10]. Hence it is permissible to utilize the same non-linear switching characteristic for each of the three gaps in the equivalent circuit of the CX1171 thyratron.

Cdrift in Fig. 2 represents the drift space capacitance. Cdrift is in the range 25pF to 30pF for the CX1171 thyratron[10]: 30pF has been used for simulating the thyratron. Cgnd in Figs. 2 and 3 represents the parasitic capacitance from the grading ring to ground. The value

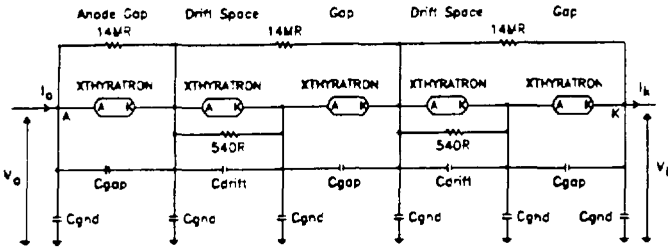

Figure 2: Three gap thyratron: drift-spaces simulated

of this capacitance affects the predicted cathode displacement current (see Fig. 4).

Scaling a typical measured pulse (Fig. 2 of reference [1]), from a pulse generator borrowed from CERN PS Division, to correspond with a PFN pre-charge of 80kV, gives 31A and 72A, respectively, for the first and second peak of cathode displacement current. Assuming a value of τ_1 of 7ns, which gives a predicted cathode current rise-time of about 32ns (see above):

- when Cgnd=10.6pF, the 3-gap thyratron model with drift spaces (Fig. 2) results in a similar magnitude of predicted cathode displacement current (Fig. 4) [37A and 72A for the first and second peaks, respectively], to the measured current;
- when Cgnd=9.4pF, the 3-gap thyratron model with drift spaces lumped with the cathode and central gaps (Fig. 3) results in an almost identical magnitude of predicted cathode displacement current [32A and 72A for the first and second peaks, respectively], to the measured current.

Where drift-spaces are simulated the delay between a gap turning-on and the associated drift-space 'turning-on' is assumed to be half of the delay between consecutive gaps turning-on: this assumption is consistent with measurements of anode delay times for two different grid connections[10].

Fig. 5 shows predicted anode and cathode displacement current when the equivalent circuit shown in Fig. 2 is utilized: the cathode displacement current is significantly greater in magnitude than the anode displacement current. τ_1 for the thyratron model is assumed to be 7ns, and in order to err on the pessimistic side a value of 12pF, rather than 10.6pF, is assumed for Cgnd. Unless stated otherwise τ_1=7ns and Cgnd=12pF are utilized for the remainder of the predictions reported in this paper. In addition, unless stated otherwise, the equivalent circuit shown in Fig. 2 is utilized for the thyratron.

When the simulated time-constant τ_1 is greater than 4ns the equivalent circuit of Fig. 3 results in similar predictions to those obtained when using the equivalent circuit of Fig. 2. However for a simulated time constant of less than 4ns (corresponds to a 10% to 90% current rise-time of about 17ns when magnetic assistance is not used) there is also a significant displacement current flow associated with the 'turn-on' of the drift-spaces, and therefore it is necessary to utilize the equivalent circuit shown in Fig. 2. Hence for $\tau_1 \simeq$7ns the simplified circuit of Fig. 3 may be utilized for simulating a CX1171 thyratron, as there is a reduction in CPU time but little loss in accuracy.

Validation of Mathematical Model of Thyratron

An investigation of switching loss of a CX1171A thyratron[8] is reported in reference[4]. The thyratron under test, in reference[4], was installed in a system with a characteristic impedance (Z_0) of 15Ω, with the thyratron cathode at negative high voltage. Parasitic capacitance of the isolating transformer and grid drive components of the cathode region resulted in a 40% initial overshoot of anode current[4]. Fig. 1 of reference[4] shows the test circuit used for investigating switching loss; Fig. 6 of this paper shows the basic circuit simulated for comparing predictions with measurements reported in reference[4]. C_k in Fig. 6 represents the parasitic capacitance associated with the cathode region. A value of 500pF for C_k results in an overshoot of 40% in the predicted anode current, hence 500pF was used for the remainder of the investigations to validate the mathematical model of the thyratron.

As per the investigations reported in reference[4], thyratron loss is determined from $\int([V_a - V_k] \times I_a)dt$, where (see Figs. 2 and 3):

- V_a is instantaneous anode voltage;
- V_k is instantaneous cathode voltage;
- I_a is instantaneous anode current.

The integration is carried out from pre-pulse current zero to post-pulse current zero, and conduction loss is subtracted from the resultant energy loss. Integrating over this period of time 'neutralizes' the reactive energy which is stored in the parasitic inductance while the thyratron is carrying load current[4].

The predicted sum of switching and conduction losses, for a PFN pre-charge of 80kV, is 3.0J; subtracting a conduction loss of 0.2J results in a predicted switching loss of 2.8J, which is in excellent agreement with the 2.8J reported in reference[4]. The integral $\int([V_a - V_k] \times I_a)dt$ assumes that the measured anode current is simultaneously flowing through the three gaps and two drift spaces. A detailed analysis of the predicted power dissipation in each of the gaps and drift spaces, where the energy dissipation for each gap and drift space is calculated from the predicted instantaneous voltage drop associated with the gap or drift space and the instantaneous current through the same gap or drift space, indicates that the integral $\int([V_a - V_k] \times I_a)dt$ overestimates energy dissipation in the thyratron by approximately 0.3J per pulse. Approximately 80% of the predicted switching loss, where the total loss is calculated from $\int([V_a - V_k] \times I_a)dt$, is associated with the anode gap: measurements indicated that about 70% of the total loss is associated with the anode gap[4]. The predictions show that the peak power dissipation in the anode gap (35MW) is almost a factor of 20 greater than the peak dissipation in any of the other

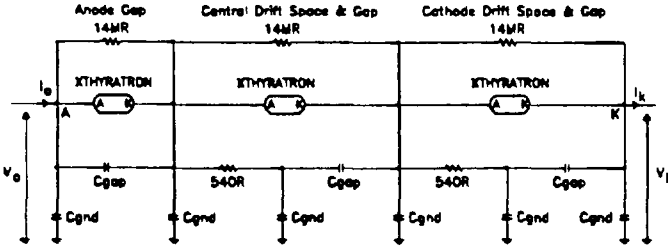

Figure 3: Three gap thyratron: drift-spaces lumped with cathode and central gaps

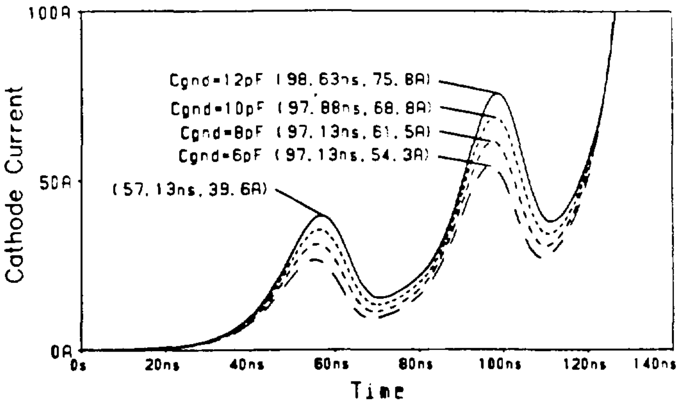

Figure 4: Effect of the value of Cgnd upon predicted cathode displacement current. Z_0=30Ω, V_{PFN}=80kV

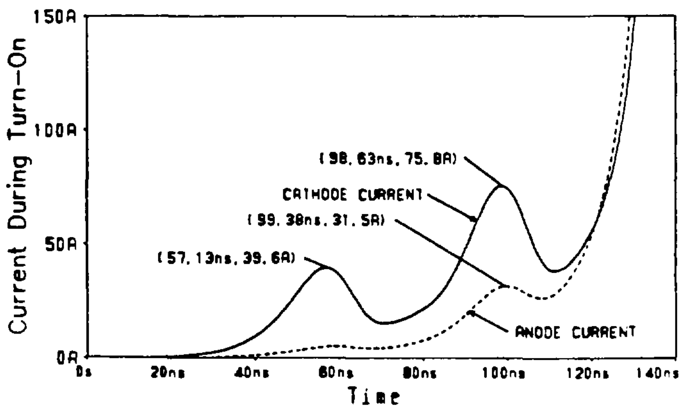

Figure 5: Predicted anode and cathode displacement current. Z_0=30Ω, V_{PFN}=80kV

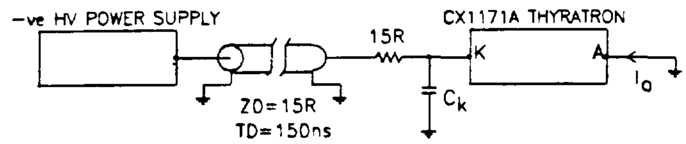

Figure 6: Block diagram of test circuit used in reference[4]

gaps or drift spaces.

Subsequently, a saturating inductor consisting of 72cm^2 of CMD5005 ferrite[11] was simulated as being connected adjacent to the anode of the thyratron. A linear inductor was modelled in series with the saturating inductor, to give a total saturated inductance of 370nH[4]. The predicted sum of switching and conduction losses, calculated from $\int([V_a - V_k] \times I_a)dt$ for a PFN pre-charge of 80kV, is 0.74J; subtracting conduction losses of 0.21J results in a predicted switching loss of about 0.5J, which is in good agreement with the 0.4J reported in reference[4]. A detailed analysis of the predicted dissipation indicates that, for this case, the integral $\int([V_a - V_k] \times I_a)dt$ overestimates energy dissipation in the thyratron by approximately 0.15J per pulse. Approximately 40% of the predicted switching loss, where the total loss is calculated from $\int([V_a - V_k] \times I_a)dt$, is associated with the anode gap. The predictions show that the peak power dissipation in the anode gap (8MW) is almost a factor of 3 greater than the peak dissipation in any of the other gaps or drift spaces. Hence the saturating inductor has reduced the predicted energy loss during switching by a factor of approximately 5.5, and reduced the peak power dissipation by a factor of about 4.5.

Unless stated otherwise, the remainder of the investigations reported in this paper assume a system with a characteristic impedance of 30Ω (as per the prototype TRIUMF kicker magnet), with the thyratron anode connected to a positively charged PFN (see Fig. 7). In addition the PFN pre-charge is simulated as 80kV.

Predicted Thyratron Dissipation

Fig. 7 shows the circuit simulated to investigate the effect of saturating ferrites upon predicted switching losses for the TRIUMF 30Ω system. A switching loss reduction saturating inductor (S.L.S.I.) is connected to the anode of the thyratron, as this helps to reduce the effect of anode displacement current upon the field in the kicker magnet (see below).

The S.L.S.I. is assumed to be manufactured from split toroidal cores of CMD5005 ferrite[11]. An air gap of 0.04mm is included to reduce the remanent flux density in the ferrite. The inner and outer diameters for the switching loss ferrite have been chosen to be 1 cm and 10 cm respectively[4]. The ferrite is assumed to be housed in a cylindrical aluminium housing with an inside diameter of 12cm. In order to calculate end-to-end capacitance, and capacitance to the aluminium housing, the relative permittivity of the ferrite is assumed to be 15. The magnetic cross-sectional area (CSA) of the ferrite is swept through a range of values.

Fig 8 shows a plot of the predicted switching loss within the thyratron, for capacitances from thyratron cathode to ground of 20pF and 500pF. A S.L.S.I. with a magnetic CSA of 72cm^2 reduces switching loss by a factor of about 3, in comparison with no S.L.S.I.. As the magnetic CSA of the S.L.S.I. is increased beyond 80 cm^2 there is little further reduction in the thyratron switching loss.

Predicted Thyratron Pre-Pulse Current

No S.L.S.I.'s Simulated

Anode and cathode displacement current are fairly insensitive to the characteristic impedance of the system[12]. Similarly the magnitude of the anode and cathode displacement current are virtually independent of the magnitude of stray capacitance from thyratron cathode to ground[12]. However the energy dissipated within the thyratron is dependent upon both the stray capacitance from cathode to ground (Fig. 8) and the characteristic impedance of the system[12].

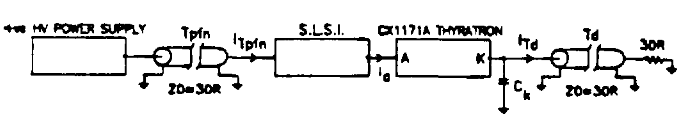

Figure 7: Block diagram of circuit used to investigate switching loss and pre-pulse current.

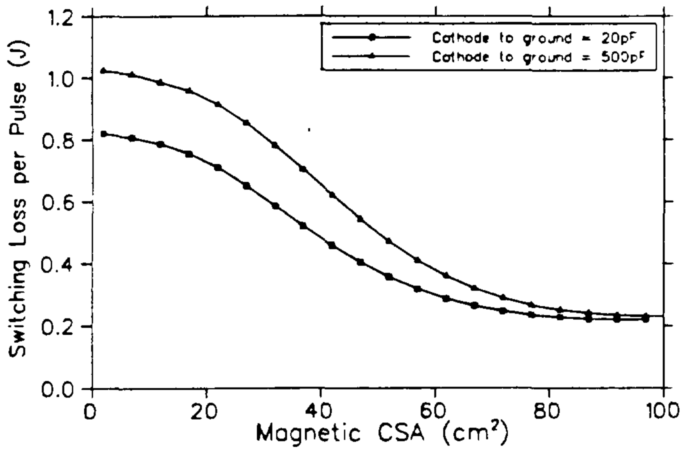

Figure 8: Predicted dissipation in thyratron. Z_0=30Ω, V_{PFN}=80kV

S.L.S.I.'s Simulated

If a S.L.S.I. is connected adjacent to either the cathode or the anode (see Fig. 7) of the thyratron, all of the cathode or anode displacement current does not necessarily flow into the transmission cable Td (Fig. 9) or PFN cable (see Fig. 10). Pre-pulse current I_{Td} effects the pre-pulse kick, whereas pre-pulse current I_{Tpfn} effects the back-end of the flat-top of the kick.

Fig. 9 shows a plot of predicted cathode current for situations without a S.L.S.I. and with a S.L.S.I. with a magnetic CSA of 72 cm^2 connected firstly adjacent to the thyratron anode, and subsequently adjacent to the thyratron cathode. Fig. 10 shows a plot of predicted anode current for situations without a S.L.S.I. and with a S.L.S.I. with a magnetic CSA of 72 cm^2 connected firstly adjacent to the thyratron anode, and subsequently adjacent to the thyratron cathode.

The presence of the S.L.S.I. adjacent to the cathode does not significantly modify PFN current I_{Tpfn} up to an elapsed time of 110ns (Fig. 10). However there is a significant second peak of pre-pulse PFN current introduced, of approximately 410A, at an elapsed time of about 147ns (Fig. 10). The S.L.S.I. adjacent to the cathode does however significantly reduce the magnitude of the pre-pulse current I_{Td} flowing into the transmission cable [Fig. 9].

The presence of the S.L.S.I. adjacent to the anode does not significantly modify current I_{Td} flowing into the transmission cable up to an elapsed time of 110ns (Fig. 9). However it introduces a third peak of pre-pulse current I_{Td}, flowing into the transmission cable, of approximately 154A at about 143ns elapsed time (Fig. 9).

The above predictions for pre-pulse currents I_{Td} and I_{Tpfn} indicate that, when a good fall-time is required for the kick, it is preferable to connect the S.L.S.I. adjacent to the PFN side of the thyratron. For example, as in this study, when the thyratron is anode connected to a positively charged PFN the optimum position for the S.L.S.I. is adjacent to the anode of the thyratron. Connecting the S.L.S.I. adjacent to the anode reduces the effect of the pre-pulse current flowing from the PFN, upon the flat-top kick. Pre-pulse current I_{Tpfn} has a peak value of about 32A (2.4% of load current) both without a S.L.S.I. present and with a S.L.S.I. connected adjacent to the thyratron anode. With a S.L.S.I. connected adjacent to the thyratron cathode,

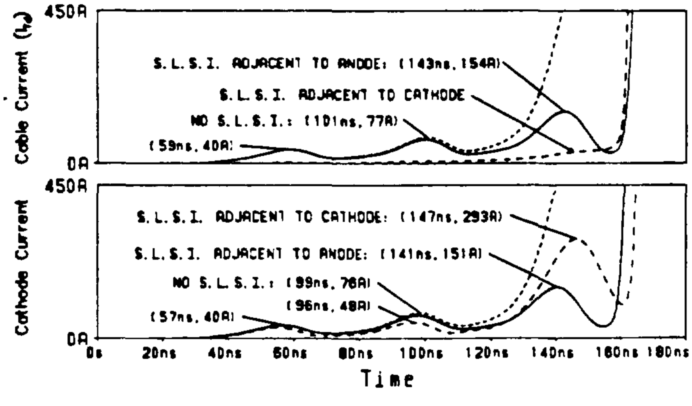

Figure 9: Effect of S.L.S.I. upon predicted pre-pulse cathode current.

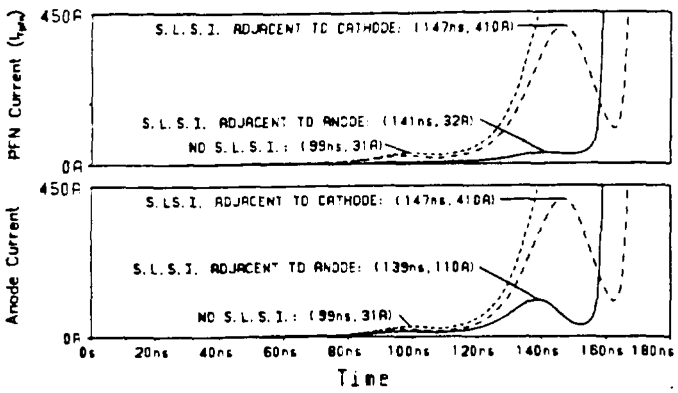

Figure 10: Effect of S.L.S.I. upon predicted pre-pulse anode current.

the pre-pulse current flowing from the PFN has a peak value of 410A (30.7% of load current).

The pre-pulse current $I_{T_{pfn}}$, introduced by connecting the S.L.S.I. adjacent to the thyratron cathode, upon flat-top kick, cannot be significantly reduced by connecting another saturating inductor elsewhere in the circuit (Fig. 1 of reference[13] shows a block diagram of the proposed kicker magnet system), for example:

- an unsaturated saturating inductor connected part-way along the PFN cable would reflect the anode pre-pulse current from the main-switch thyratron towards the kicker magnet, which would affect the flat-top of the kick;
- a saturated saturating inductor, connected part-way along the PFN cable, would not prevent the anode pre-pulse current from the dump-switch thyratron from reaching the kicker magnet; this pre-pulse current would affect the flat-top of the kick;
- a saturating inductor connected near the input to the kicker magnet would be carrying load current (i.e. saturated) when the pre-pulse anode current reached it, and hence this saturating inductor would not significantly reduce the effect of pre-pulse anode current upon the flat-top of the kick.

The effect upon pre-pulse kick of pre-pulse current I_{T_d}, introduced by connecting the S.L.S.I. adjacent to the thyratron anode, can be significantly reduced by connecting a displacement current suppression saturating inductor (D.I.S.I.) near to the input of the kicker magnet (see Fig. 1 of reference[13]). The D.I.S.I. consists of split toroidal cores manufactured from CMD5005 ferrite[11], placed over a central conductor[14]. The inner and outer diameters chosen for this ferrite are 4 cm and 6 cm, respectively.

Fig. 11 shows the predicted time response for the TRIUMF 30Ω prototype kicker magnet connected in a representative equivalent circuit, together with speed-up networks[13], S.L.S.I.'s and a D.I.S.I.. An equivalent circuit of a three gap thyratron is also modelled.

Beam impedance measurements have been carried out for the KAON factory prototype kicker magnet. These measurements indicate that the D.I.S.I. has a beneficial effect upon the longitudinal beam impedance of a kicker magnet[15].

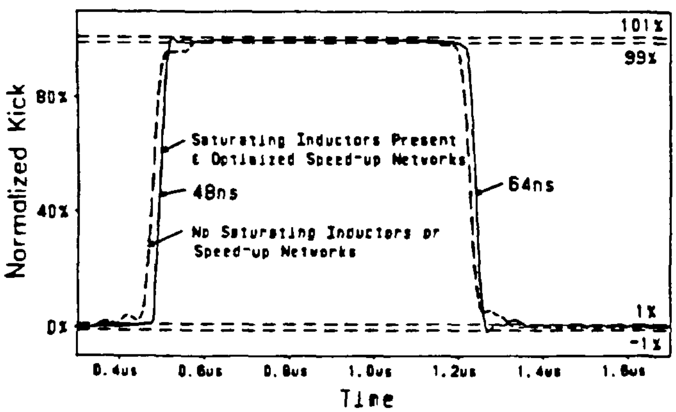

Figure 11: Predicted normalized kick for the TRIUMF prototype kicker magnet, with and without the proposed improvements

Conclusion

Two mathematical models of a three gap thyratron have been developed to simulate turn-on. One of the mathematical models simulates non-linear switching characteristics for the three gaps and two drift spaces separately, whereas the other model lumps the non-linear switching characteristics for the drift spaces with those of the cathode and central gaps. In general, for 10% to 90% current rise-times of greater than about 17ns, the model which lumps the drift spaces with the cathode and central gaps is adequate. The mathematical model, which simulates the two drift spaces separately, has been validated by comparing predicted switching losses, with and without a saturating inductor present, with switching losses measured at CERN: the agreement is good.

The mathematical model of the thyratron has been used to assess the effect of a S.L.S.I. upon pre-pulse current, and energy dissipation per pulse within the thyratron. The optimum position for a S.L.S.I. is adjacent to the PFN side of the thyratron. A S.L.S.I. with a magnetic CSA of $70cm^2$ significantly reduces switching losses in the thyratron. As the magnetic CSA is increased beyond $80cm^2$ there is not any further significant reduction in switching loss. The S.L.S.I. can also be used to reduce kick rise time. A separate D.I.S.I., connected on the input to the kicker magnet, is effective at reducing the effect of pre-pulse cathode current upon the pre-pulse kick. These improvements are presently being carried out to the borrowed CERN pulser.

Acknowledgements

The authors wish to acknowledge the useful technical discussions with both David Fiander, formerly of CERN PS Division, and staff of English Electric Valve Company.

References

[1] M.J. Barnes, G.D. Wait, "Kickers for the Kaon Factory" Proceedings of XVth International Conference of High Energy Accelerators (HEACC'92), Hamburg, July 1992.

[2] "TRIUMF KAON FACTORY STUDY," *Accelerator Design Report*, May 1990.

[3] D. Fiander, K. Metzmacher and P. Pearce, Kickers and Septa at the PS Complex, CERN. Proceedings of the KAON PDS Magnet Design Workshop, October 1988, pp 71-79.

[4] L. Ducimetiere, D.C. Fiander "Commutation Losses of a Multigap High Voltage Thyratron". IEEE Conference Record of the 1990 Nineteenth Power Modulator Symposium, June 26-28, 1990, San Diego, pp248-253.

[5] R.L. Cassel, T.S. Mattison "Kicker Prepulse Canceller". IEEE Conference Record of the 1991 Particle Accelerator Conference, May 6-9, 1991, pp3162-3164.

[6] M.J. Barnes, G.D. Wait, "Improving the Performance of Kicker Magnet Systems" Proceedings of XVth International Conference of High Energy Accelerators (HEACC'92), Hamburg, July 1992.

[7] Microsim Corporation, 20 Fairbanks, Irvine, California. U.S.A. Tel. (714) 770 3022.

[8] Hydrogen Thyratrons (Product Data), English Electric Valve Co., Chelmsford, Essex, U.K..

[9] Private Communication with V. Sandberg, LAMPF, Los Alamos, New Mexico, USA.

[10] Private Communication with R. Sheldrake, English Electric Valve Co., Chelmsford, Essex, U.K..

[11] Engineered Ferrites (Product Data), Ceramic Magnetics Inc., New Jersey, USA. Publication 10M 3/88.

[12] M.J. Barnes, G.D. Wait, "Effect of Saturating Ferrites for the 30Ω, Resistively Terminated, Prototype Kicker Magnet". TRI-DN-91-K192.

[13] M.J. Barnes, G.D. Wait, "Optimization of Speed-Up Network Component Values for the 30Ω Resistively Terminated Prototype Kicker Magnet", Proceedings of the 1993 Particle Accelerator Conference (PAC93), Washington, May 1993.

[14] M.J. Barnes, G.D. Wait, "Suppression of the Effect of Thyratron Displacement Current upon the Field in the 30 Ω Prototype Kicker Magnet". TRI-DN-91-K170.

[15] H.J. Tran, M.J. Barnes, G.D. Wait, Y. Yin, "Longitudinal Impedance of a Prototype Kicker Magnet", Proceedings of the 1993 Particle Accelerator Conference (PAC93), Washington, May 1993.